Immunisation of ferrets and mice with recombinant SARS-CoV-2 spike protein formulated with Advax-SM adjuvant protects against COVID-19 infection

Lei Li [a,b,1], Yoshikazu Honda-Okubo [a,b,1], Ying Huang [c], Hyesun Jang [c], Michael A. Carlock [c], Jeremy Baldwin [a], Sakshi Piplani [a,b], Anne G. Bebin-Blackwell [c], David Forgacs [c], Kaori Sakamoto [e], Alberto Stella [f], Stuart Turville [f], Tim Chataway [b], Alex Colella [b], Jamie Triccas [g], Ted M. Ross [c,d,2], Nikolai Petrovsky [a,b,*,2]

[a] Vaxine Pty Ltd., Bedford Park, Adelaide 5042, SA, Australia
[b] College of Medicine and Public Health, Flinders University, Adelaide 5042, SA, Australia
[c] Center for Vaccines and Immunology, University of Georgia, Athens, GA, USA
[d] Department of Infectious Diseases, University of Georgia, Athens, GA, USA
[e] Department of Pathology, University of Georgia, Athens, GA, USA
[f] Centre for Virus Research, Westmead Millennium Institute, Westmead Hospital and University of Sydney, Sydney 2145, NSW, Australia
[g] School of Medical Sciences and Marie Bashir Institute, University of Sydney, Sydney, NSW 2006, Australia

ARTICLE INFO

ABSTRACT

The development of a safe and effective vaccine is a key requirement to overcoming the COVID-19 pandemic. Recombinant proteins represent the most reliable and safe vaccine approach but generally require a suitable adjuvant for robust and durable immunity. We used the SARS-CoV-2 genomic sequence and *in silico* structural modelling to design a recombinant spike protein vaccine (Covax-19™). A synthetic gene encoding the spike extracellular domain (ECD) was inserted into a baculovirus backbone to express the protein in insect cell cultures. The spike ECD was formulated with Advax-SM adjuvant and first tested for immunogenicity in C57BL/6 and BALB/c mice. Covax-19 vaccine induced high spike protein binding antibody levels that neutralised the original lineage B.1.319 virus from which the vaccine spike protein was derived, as well as the variant B.1.1.7 lineage virus. Covax-19 vaccine also induced a high frequency of spike-specific CD4 + and CD8 + memory T-cells with a dominant Th1 phenotype associated with the ability to kill spike-labelled target cells *in vivo*. Ferrets immunised with Covax-19 vaccine intramuscularly twice 2 weeks apart made spike receptor binding domain (RBD) IgG and were protected against an intranasal challenge with SARS-CoV-2 virus given two weeks after the last immunisation. Notably, ferrets that received the two higher doses of Covax-19 vaccine had no detectable virus in their lungs or in nasal washes at day 3 post-challenge, suggesting that in addition to lung protection, Covax-19 vaccine may have the potential to reduce virus transmission. This data supports advancement of Covax-19 vaccine into human clinical trials.

© 2021 Elsevier Ltd. All rights reserved.

1. Introduction

COVID-19 is caused by lung infection with severe acute respiratory syndrome coronavirus-2 (SARS-CoV-2) [1]. To date, there have been over 190 million reported COVID-19 cases in over 215 countries with greater than 4.1 million confirmed deaths [2]. SARS-CoV-2 causes a constellation of clinical outcomes from asymptomatic infection to respiratory failure and death [3]. Although public health strategies, such as social distancing, masks and quarantine, have helped control virus transmission, many countries are experiencing second and third waves of cases [4] including with virus variants of concern with increased virulence [5]. Global efforts are currently underway to develop COVID-19 vaccines [6] including live virus vectors, inactivated viruses, nucleic acids (DNA or RNA) and recombinant proteins [7]. Although several vaccines have received emergency-use authorisation, ongoing questions include likely duration of vaccine protection, long-term safety, potential for antibody-enhanced disease, activity against variant strains and immune correlates of vaccine protection [8-10].

Recombinant or inactivated protein vaccines are a safe and reliable approach but generally suffer from weak immunogenicity unless formulated with an appropriate adjuvant [11]. Adjuvants induce higher and more durable immune responses and can also be used to impart a relevant T helper bias to the immune effector response [12] and can overcome immune impairment seen with advancing age or chronic disease [13]. Advax-SM is a combination adjuvant developed by our team that consists of delta inulin polysaccharide particles (Advax™) formulated with a Toll-like receptor 9 (TLR9)-active oligonucleotide, CpG55.2. A similar adjuvant approach provided enhanced protection of recombinant spike protein vaccines against severe acute respiratory syndrome (SARS) and Middle East respiratory syndrome (MERS), coronaviruses [14,15]. The Th1-bias imparted by the adjuvant also prevented the eosinophilic lung immunopathology otherwise seen after immunisation with SARS spike protein alone or with alum adjuvant [14]. Advax adjuvant has been shown to be safe and effective in human vaccines against seasonal and pandemic influenza [16,17] and hepatitis B [18].

Advanced computer modelling techniques may be useful to accelerate pandemic vaccine design. This study describes how we used a range of approaches including computer modelling to characterise the SARS-CoV-2 spike protein from the genomic sequence, and then used a modelled 3-D structure to identify angiotensin converting enzyme 2 (ACE2) as the relevant human receptor. We then utilised our computer model to design a vaccine from the extracellular domain (ECD) of the SARS-CoV-2 spike protein and tested whether this antigen when formulated with Advax-SM adjuvant would induce neutralising antibodies able to block the binding of SARS-CoV-2 virus to ACE2 thereby preventing infection. While our study was in progress others confirmed that ACE2 was the receptor for the spike protein and viral entry into host cells was further enhanced by priming of the spike protein by transmembrane protease serine 2 (TMPRSS2) [19]. Our subsequent results confirmed that our computationally-designed spike antigen when formulated with Advax-SM adjuvant induced antibodies against spike protein that were able to neutralise wildtype lineage B.1.319 SARS-CoV-2 virus as well as cross neutralising the variant B.1.1.7 lineage virus. Covax-19 vaccine induced memory CD4 and CD8 T cell responses with a Th1 phenotype and this translated into the ability to kill spike-labelled target cells *in vivo*. Notably, Covax-19 vaccine provided lung protection in immunised ferrets but also inhibited day 3 nasal virus shedding, suggesting an additional potential to impact on virus transmission.

2. Methods

2.1. Vaccine design

In mid-January 2020, we identified the putative spike protein from the SARS-CoV-2 genome sequence in NCBI (accession number: NC 045512) [20]. Given the homology of the spike proteins (76.4% sequence identity), SARS-CoV-1 was used as a template to model the SARS-CoV-2 spike protein. We performed a PSI-BLAST search against the Protein Data Bank (PDB) Database for 3D modelling template selection. Using the SARS-CoV-1 structure (PDB-ID 6ACC) [21] we performed structural homology modelling using Modeller9.23 (https://salilab.org/modeller/) to obtain a 3D structure of SARS-CoV-2 spike protein (Fig. 1A). The quality of the spike protein model was evaluated using GA341 and DOPE score, and the model was assessed using the SWISS-MODEL structure assessment server (https://swissmodel.expasy.org/assess). To help identify the putative cellular receptor for SARS-CoV-2, the crystal structure of human ACE2 (PDB-ID 3SCI) [22] was retrieved, and using HDOCK server, the spike protein was then docked against human ACE2

protein (http://hdock.phys.hust.edu.cn/) [23]. The docking poses were ranked using an energy-based scoring function and the docked structure analysed using UCSF Chimera. The high binding score predicted human ACE2 as the entry receptor for SARS-CoV-2 spike protein, confirming spike protein suitability for vaccine design [24]. The docked model was optimised using AMBER99SB-ILDN force field in Gromacs2020 (https://www.gromacs.org/). Molecular dynamic simulation (MDS) was carried out for 100 ns using a GPU-accelerated version of the program (**Supplementary video 1**). The structural stability of the complex was monitored by the root-mean-square deviation (RMSD) value of the backbone atoms of the entire protein. The free energy of binding was calculated for simulated SARS-CoV-2 Spike and humanACE2 structure using g_MMPBSA. Finally, MDS was performed on the spike protein ECD vaccine construct to assess its ability to form a stable trimer despite the lack of the transmembrane and cytoplasmic domains. The insect cell codon-optimised expression cassette was cloned into pFASTBac1, and baculovirus was generated following standard Bac-to-Bac procedures. Recombinant baculovirus was expanded in Sf9 cells to P3 and then used for infection of Trichoplusia ni High five cells (Thermo Fisher, USA) for protein expression. At 72 h post infection, the culture supernatant was clarified by centrifugation, and then the recombinant spike protein ECD was purified by HisTrap Excel column using the AKTA chromatography system, concentrated by ultrafiltration and buffer changed to phosphate buffered saline (PBS) then terminally filter sterilised. The sequence of the recombinant spike protein (rSp) was confirmed by mass spectroscopy, SDS-PAGE gels and Western blots. Endotoxin was measured using a PyroGene™ Endotoxin Detection System (Cat. No. 50-658U, LONZA, Walkersville, MD, USA), and residual DNA content in the final vaccine product was also measured using a Quant-iT™ PicoGreen™ dsDNA Assay Kit (ThermoFisher, P7589) following manufacturer's instructions.

2.2. Mouse immunisation protocol

Female, BALB/c and C57BL/6 (BL6) mice (6–10 weeks old) were supplied by the central animal facility of Flinders University. Mice were immunised intramuscularly (i.m.) with 1 or 5 μg rSp alone or mixed with either 1 mg Advax-SM adjuvant or where indicated 50 μg Al(OH)$_3$ (2% Alhydrogel, Croda Denmark) in the thigh muscle at weeks 0 and 2. Blood samples were collected by cheek vein bleeding at 2 weeks after each immunisation. Serum was separated by centrifugation and stored at − 20C prior to use. Advax-SM (Vaxine, Adelaide, Australia) was a sterile suspension of delta inulin microparticles at 50 mg/ml with CpG55.2 at 0.5 mg/ml.

2.3. Antigen-specific ELISA for murine studies

Spike-specific antibodies were determined by ELISA. Briefly, 1 μg/ml rSp [corresponding to SARS-CoV-2 (Wuhan) reference sequence Q13 to P1209] or 2 μg/ml receptor-binding domain (RBD) [corresponding to SARS-CoV-2 (Wuhan) reference sequence R319 to F541] antigen in PBS were used to coat 96-well ELISA plates. After blocking, 100 μL of diluted serum samples were added followed by biotinylated anti-mouse IgG (Sigma-Aldrich), IgG1, IgG2a/c, IgG2b, IgG3 and IgM antibodies (all from Abcam) with horseradish peroxidase (HRP)-conjugated Streptavidin (BD Biosciences) for 1 h (h). After washing, 100 μL of TMB substrate (KPL, SeraCare, Gaithersburg, MD, USA) was added and incubated for 10 min before the reaction was stopped with 100 μL 1 M Phosphoric Acid (Sigma-Aldrich). The optical density was measured at 450 nm (OD$_{450}$ nm) using a VersaMax plate reader (Molecular Devices, LLC., San Jose, CA, USA) and analysed using SoftMax Pro Software. Average OD$_{450}$ nm values obtained from negative control wells were subtracted.

A.

B.

Human ACE2

SARS-CoV-2 RBD

C.

RMSD
Protein after 1sq fit to protein
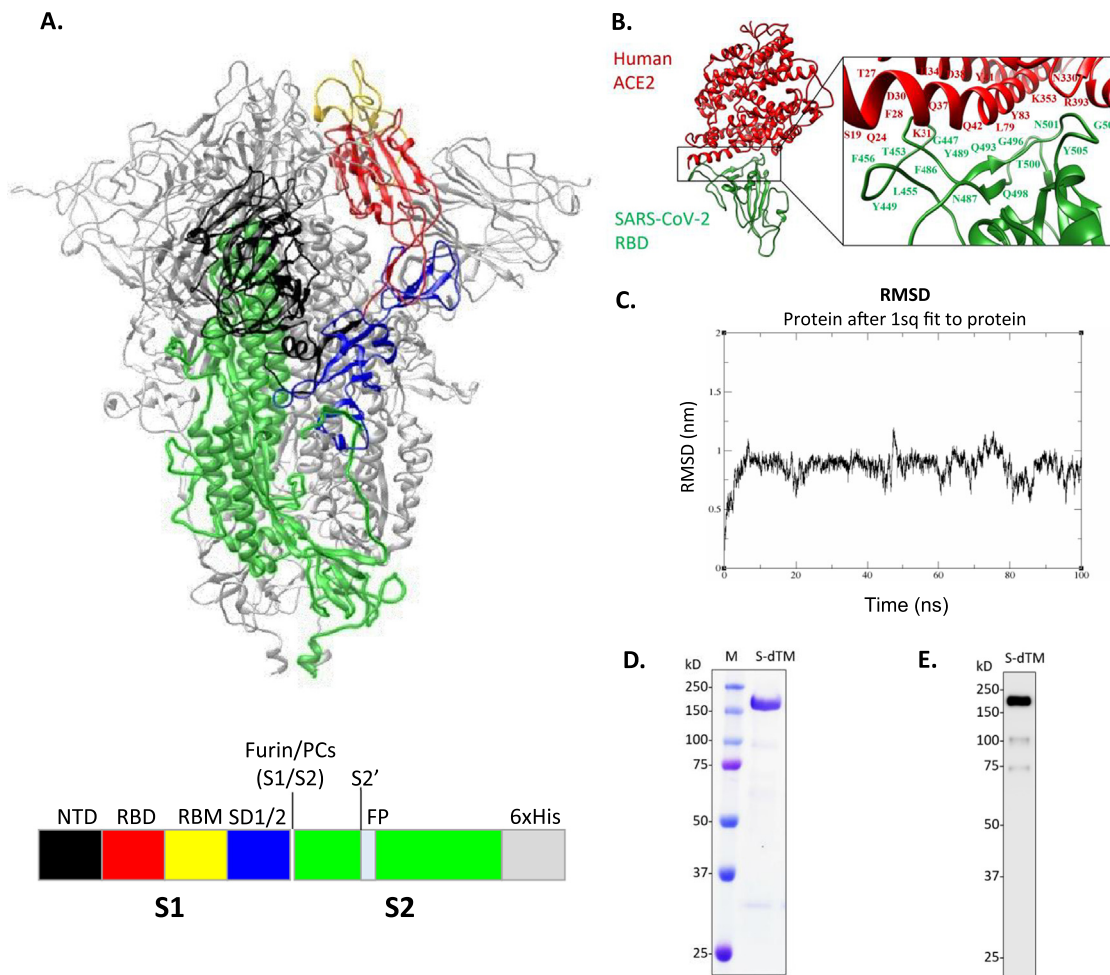
D.

E.

Fig. 1. Modelling and expression of SARS-CoV-2 spike ectodomain (ECD) vaccine antigen. (A) Diagram of the ECD construct of SARS-CoV-2 spike (S) protein. Honeybee melittin signal (HBMss) peptide was used for efficient secretion expression. Transmembrane domain and intracellular domain were removed and replaced with a TEV cleavage site followed by 6x Histidines (6xHis). (B) SARS-CoV-2 receptor binding domain (RBD) (green) binding human Angiotensin-Converting Enzyme 2 (ACE2) (red). (C) Molecular dynamic simulation (MDS) run for 100 ns showed the structure was stable. (D) Representative Coomassie Brilliant Blue stained SDS-PAGE of purified S-dTM. (E) Purified S-dTM was confirmed by Western blot using anti-SARS-CoV-2 spike mouse polyclonal antibody. (For interpretation of the references to colour in this figure legend, the reader is referred to the web version of this article.) (For interpretation of the references to colour in this figure legend, the reader is referred to the web version of this article.)

2.4. High-throughput SARS-CoV-2 live virus neutralisation assay

A high-content microscopy approach was used to assess the ability of mice sera to inhibit SARS-CoV-2 viral infection and the resulting cytopathic effect in live permissive cells. Briefly, serum samples were diluted in cell culture medium (MEM-2% FCS) to create a 2-fold dilution series (e.g. 1:20 to 1:160). Each dilution was then mixed (in duplicate) with an equal volume of virus solution (B.1.319 or B.1.1.7 strains) at 8×10^3 $TCID_{50}$/ml (so that dilution series becomes 1:40–1:320), followed by 1 h incubation at 37 °C. Meanwhile, freshly trypsinised VeroE6 cells were and plated in 384-well plates (Corning #CLS3985) at 5×10^3 cells per well in 40 μL. After 1 h of virus-serum coincubation, 40 μL were added to the cell-plate for a final well volume of 80 μL. Plates were incubated for 72 h until readout (37 °C, 5% CO_2, greater than90% relative humidity), which occurred by staining cellular nuclei with NucBlue dye (Invitrogen, #R37605) and imaging the entire well's area with a high-content fluorescence microscopy system (IN Cell Analyzer 2500HS, Cytiva Life Sciences). The number of cells per well was determined using InCarta image analysis software (Cytiva). The percentage of viral neutralisation for each well was calculated with the formula N = (D-(1-Q))x100/D, where "Q" is

the well's nuclear count divided by the average nuclear count of the untreated control wells (i.e. without virus or serum), and "D" equals 1 minus the average Q-value for the positive infection control wells (i.e. cells + virus, without serum). Therefore, the average nuclear counts for the infected and uninfected cell controls are defined as 0% and 100% neutralisation levels, respectively. The threshold for determining the neutralization endpoint titre of diluted serum samples mixed with virus was set to N $\geq$ 50%.

2.5. SARS-CoV-2 spike pseudotyped neutralisation assay

A non-replicative SARS-CoV-2 Spike pseudotyped lentivirus-based platform was developed to evaluate neutralisation activity in infected/convalescent sera in a Biosafety Level 2 (BSL2) facility. The human ACE2 open reading frame (Addgene# 1786) was cloned into a 3rd generation lentiviral expression vector pRRLSIN.cPPT. PGK-GFP.WPRE (Addgene# 122053), and clonal HEK 293 T cells stably expressing ACE2 were generated by lentiviral transductions as described previously [25], followed by single cell sorting into 50% HEK 293 T conditioned media (media conditioned from 50% confluent HEK 293 T cultures). Lentiviral particles pseudotyped with SARS-CoV2 Spike envelope were produced by co-

transfecting HEK 293 T cells with a GFP encoding 3rd generation lentiviral plasmid HRSIN-CSGW (a gift from Camille Frecha [26]), psPAX2 and plasmid expressing codon optimised but C-terminal truncated SARS-CoV-2 S protein (pCG1-SARS-2-S Delta18 [19], herein Spike Delta18) courtesy of Professor Stefan Polhman using polyethylenimine as described previously [25]. Neutralisation activity of donor sera was measured using a single round transduction of ACE2-HEK 293 T with Spike pseudotyped lentiviral particles. Briefly, virus particles were pre-incubated with serially diluted donor sera for 1 h at 37 °C. Virus-serum was then added onto ACE2-HEK 293 T cells seeded at 2,500 cells per well in a 384-well tissue culture plate a day before. Following spinoculation at 1200xg for 1 h at 18 °C, the cells were moved to 37 °C for a further 72 h. Entry of pseudotyped particles was assessed by imaging GFP-positive cells and total cell numbers imaged through live nuclei counter staining using NucBlue (Invitrogen). Total cell counts and % GFP-positive cells were acquired using the InCell imaging platform followed by enumeration with InCarta high content image analysis software (Cytiva). Neutralisation was measured by reduction in % GFP expression relative to control group infected with the virus particles without any serum treatment.

2.6. Murine T-cell response

BALB/c and BL6 mice were sacrificed, and individual spleens were collected one to two weeks after the last immunisation. Single-cell suspension in sterile PBS + 3% FCS was prepared using a 70 μm easy strainer (Greiner Bio-One) with a 5 ml syringe plunger. Isolated spleen cells were pelleted and incubated in red blood cell (RBC) lysis buffer. For Cytometric Bead Array (CBA) assay, splenocytes were cultured at 5×10^5 cells/well in 96-well plates with 3 μg/ml of rSp antigen [corresponding to SARS-CoV-2 (Wuhan) reference sequence Q13 to P1209] at 37 °C and 5% CO_2. Two days later, the supernatants were harvested and cytokine concentrations determined by mouse Th1/Th2/Th17 CBA (BD) and analysed by FCAP array Software (BD). In addition to CBA assay, enzyme-linked immune absorbent spot (ELISPOT) assay was performed using mouse Interlukin-2 (IL-2), Interlukin-4 (IL-4) or Interferon gamma (IFN-γ) ELISPOT set (BD PharMingen) or Interlukin-17 (IL-17) antibodies (BioLegend) according to the manufacturer's instruction. Briefly, single-cell suspensions were prepared from spleens of mice and plated in Millipore MultiScreen-HA 96-well filter plates (Millipore) pre-coated with anti-mouse IL-2, IL-4, IL-17 or IFN-γ antibodies overnight at 4 °C and blocked by RPMI-1640 containing 10% FBS. Cells were incubated for 48 h in the presence or absence of rSp protein at 37 °C and 5% CO_2. Wells were washed and incubated with biotinylated labelled anti-mouse IL-2, IL-4, IL-17 or IFN-γ antibody at room temperature (RT). After washing, wells were incubated with HRP-conjugated Streptavidin (BD Biosciences) for 1 h at RT. Wells were extensively washed again and developed with 3-amino-9-ethyl-carbazole (AEC) substrate set (BD Biosciences). After drying, spots were counted on an ImmunoSpot ELISPOT reader (CTL ImmunoSpot Reader, software version 5.1.36). Finally, a T-cell proliferation assay was performed by incubating collected mice spleen cells for 7 min at RT with 5 μM Carboxyfluorescein succinimidyl ester (CFSE) (Life Technologies), staining was quenched with FCS and splenocytes cultured at 10^6 cells/well in 96-well plates for 5 days at 37 °C in 5% CO_2 with 3 μg/ml of rSp antigen. At the end of the incubation, the cells were stained with anti-mouse CD4-PerCP-Cy5.5 and anti-mouse CD8-APC (both from BD) and analysed on a FACSCanto II (BD). T-cell proliferation was expressed as the ratio of divided daughter cells to total T-cells, expressed as a percentage, by analogy to calculation of a stimulation index in thymidine proliferation assays.

2.7. In vivo CTL assay

Functional CD8+ T cell response was determined by performing in vivo CTL assays, as described earlier [27]. Briefly, naïve syngeneic target spleen cells were left unpulsed or pulsed for 2 h in humidified CO_2 incubator at 37 °C with 5 μM H-2 K^b-restricted Sp$_{539-546}$ (VNFNFNGL) synthetic peptide [28] (DGpeptide, Hangzhou, China). Unpulsed (control) and peptide (antigen)-pulsed spleen cells were labelled with 0.5 μM CFSE (CFSE^{low}) and 5 μM CFSE (CFSE^{high}), respectively. Then, naïve syngeneic and immunised mice were adoptively transferred with 4×10^6 cells of a 1:1 mix of control-to-antigen-pulsed target spleen cells. Eighteen (18) hours later, adoptive transfer recipient mice were euthanised, their splenocytes isolated and resuspended in PBS for acquisition on a BD FACSCanto-II instrument. To evaluate the percentage of antigen-specific target cell killing, the ratio of CFSE^{high}/CFSE^{low} in survivors was compared to the ratio in transferred naive control mice.

2.8. Ferret immunisation protocol

Fitch ferrets (Mustela putorius furo, spayed female, 6 to 12 months of age), were purchased from Triple F Farms (Sayre, PA, USA). Ferrets were pair-housed in stainless steel cages (Shor-Line, Kansas City, KS, USA) containing Sani-Chips laboratory animal bedding (P. J. Murphy Forest Products, Montville, NJ, USA) and provided Teklad Global Ferret Diet (Harlan Teklad, Madison, WI, USA) and fresh water ad libitum. Groups (n = 6) were vaccinated at day 0 and boosted at day 14 with Covax-19 vaccine (12.5, 25 or 50 μg) formulated with 15 mg Advax-SM adjuvant. Control ferrets received either saline only (n = 3) or were immunised with influenza recombinant hemagglutinin vaccine (rH7, Protein Sciences, Meriden, USA) formulated with Advax-SM as a control. Blood was collected on days 0, 14 and 28 post-immunisation and day 10 post-challenge and stored at − 20C prior to use.

2.9. Ferret challenges

At day 28, all ferrets were infected intranasally with SARS-CoV-2 virus (1×10^5 PFU) and were monitored daily for adverse events, including weight loss and elevated temperature for 10 days. At day 3 post infection, nasal swabs were collected from all animals, and three animals from each group, except for the Advax-SM only control group, were humanely euthanised and lung tissue was collected. Three lobes from the right lung of each animal were formalin fixed for histopathology. Two lobes from the left side of lung from each animal were snap frozen and homogenised using 1 ml DMEM, and the supernatant was collected and kept frozen at − 80C for viral titres.

2.10. Ferret spike RBD-binding IgG ELISA

Immulon® 4HBX plates (Thermo Fisher Scientific, Waltham, MA, USA) were coated with 100 ng/well of recombinant SARS-CoV-2 Spike protein RBD [corresponding to SARS-CoV-2 (Wuhan) reference sequence R319 to F541] in PBS overnight at 4 °C in a humidified chamber. Plates were blocked with blocking buffer made up with 2% bovine serum albumin (BSA) Fraction V (Thermo Fisher Scientific, Waltham, MA, USA), 1% gelatin from bovine skin (Sigma-Aldrich, St. Louis, MO, USA) and 0.05% PBST (PBS with 0.05% Tween20) (Thermo Fisher Scientific, Waltham, MA, USA) at 37 °C for 90 min. Serum samples from the ferrets were initially diluted 1:50 and further serially diluted 1:3 in blocking buffer to generate a 4-point binding curve (1:50, 1:150, 1:450, 1:1350). Subsequently, the plates were incubated overnight at 4 °C in a humidified chamber. The following day, plates were washed 5 times with 0.05% PBST, and IgG antibodies were detected using horseradish

peroxidase (HRP)-conjugated goat anti-ferret polyclonal IgG detection antibody (Abcam, Cambridge, UK) at a 1:4,000 dilution for a 90 min incubation at 37 °C. Plates were washed 5 times with 0.05% PBST prior to colorimetric development with 100 μL of 0.1% 2,2′-azino-bis(3-ethylbenzothiazoline-6-sulphonic acid) (ABTS, Bioworld, Dublin, OH, USA) solution with 0.05% H_2O_2 for 18 min at 37 °C. The reaction was terminated with 50 μL of 1% (w/v) sodium dodecyl sulfate (SDS, VWR International, Radnor, PA, USA). Colorimetric absorbance at 414 nm was measured using a PowerWaveXS plate reader (Biotek, Winooski, VT, USA). The dilution curve was plotted, and the area under the curve was calculated and multiplied by 1,000 to give standard units.

2.11. Determination of virus titres in ferret nasal washes

Nasal washes were titrated in quadruplicates in Vero E6 cells. Briefly, confluent VeroE6 cells were inoculated with 2-fold serial dilutions of sample in DMEM containing 2% FBS, supplemented with 1% penicillin–streptomycin (10,000 IU/ml). At 3 days post infection (dpi), virus positivity was assessed by reading out cytopathic effects. Infectious virus titres ($TCID_{50}$/ml) were calculated from four replicates of each nasal wash using the Reed–Muench method.

2.12. Haematoxylin & eosin (H&E) and immunohistochemistry staining of ferret lungs

To assess the viral replication and pathological effect of infection, ferrets (n = 3) were euthanised 3 days post infection. The right lung lobes were taken for viral plaques, the incision was tied with surgical suture, and the lung was inflated with 10 ml formalin. Lungs were removed and placed into formalin for 1 week prior to paraffin embedding. Ferret lungs were embedded into paraffin and were cut using a Lecia microtome. Transverse 5 μm sections were placed onto Apex superior adhesive glass slides (Leica biosystem Inc, IL, USA), which were coated for a positive charge, and were processed for H&E staining. Briefly, sections were deparaffinised in xylene and hydrated using different concentrations of ethanol (100%, 95%, 80% and 75%) for 2 min each. Deparaffinised and hydrated lung sections were stained with hematoxylin (Millipore sigma, MA, USA) for 8 min at RT, differentiated in 1% acid alcohol for 10 sec, and then counterstained with eosin (Millipore sigma, MA, USA) for 30 sec. Slides were then dehydrated with 95% and 100% ethanol, cleared by xylene, and mounted using Permount® mounting media (Thermo Fisher scientific, MA, USA). Lung lesions were scored by a board-certified veterinary pathologist blinded to the study groups as follows: Alveolar (ALV) score: 1 = focal, 2 = multifocal, 3 = multifocal to coalescing, 4 = majority of section infiltrated by leukocytes; Perivascular cuffing (PVC) score: 1 = 1 layer of leukocytes surrounding blood vessel, 2 = 2–5 layers, 3 = 6 – 10 layers, 4 = greater than 10 cells thick; Interstitial Pneumonia (IP) score: 1 = alveolar septa thickened by 1 leukocyte, 2 = 2 leukocytes thick, 3 = 3 leukocytes, 4 = 4 leukocytes.

For lung immunohistochemistry, the deparaffinised and hydrated lung tissue sections were subjected to antigen retrieval by sub-boiling in 10 nM sodium citrate buffer at pH6 for 10 min and then incubated in 3% fresh-made hydrogen peroxide for 10 min to inactivate endogenous peroxidase at RT. The lung sections were blocked with 5% horse serum in PBS for 1 h at RT, incubated with SARS-CoV-2 Nucleoprotein polyclonal antibody at 1:500 dilution (Invitrogen, Carlsbad, CA, USA) overnight at 4 °C, and then incubated with biotinylated goat-antibody Rabbit IgG H&L (Abcam, Waltham, MA, USA) at 1:1000 dilution for 1 h at RT. The avidin–biotin-peroxidase complex (VectStain Standard ABC kit, Vector Laboratories, Burlingham, CA, USA) was used to localise the biotinylated antibody, and DAB (Vector Laboratories,

CA, USA) was utilised for colour development. Sections were then counterstained with hematoxylin, and then mounted using Permount® mounting media (Thermo Fisher Scientific, Waltham, MA, USA). Images were obtained by Aperio digital slide scanner AT2 (Leica biosystem, Buffalo Grove, IL, USA).

2.13. Statistical analysis

GraphPad Prism 8.3.1 for Windows was used for drawing graphs and statistical analysis (GraphPad Software, San Diego, CA, USA). The differences of antibody levels were evaluated by the Mann-Whitney test, and other differences between groups were evaluated by two-tailed Student's t-test. ANOVA with Dunnett's test was used for weight loss. Limit of detection for viral plaque titres was 50 pfu/ml. Limit of detection for neutralisation was 1:10, but 1:5 was used for statistical analysis. Geometric mean titres were calculated for neutralisation assays. For all comparisons, $p < 0.05$ was considered significant . In figures * = $p < 0.05$; ** = $p < 0.01$; and *** = $p < 0.001$. All error bars on the graphs represent standard error of the mean.

2.14. Ethics statement

The mouse studies were performed at Flinders University, Australia. The protocol was approved by the Animal Welfare Committee of Flinders University and carried out in strict accordance with the Australian Code of Practice for the Care and Use of Animals for Scientific Purposes (2013). All efforts were made to minimise animal suffering. Animals were housed in cages provisioned with water and standard food and monitored daily for health and condition. After final monitoring, all of the surviving animals were humanely euthanised. Ferret studies were performed at The University of Georgia, United States. The University of Georgia Institutional Animal Care and Use Committee approved all ferret experiments, which were conducted in accordance with the National Research Council's Guide for the Care and Use of Laboratory Animals, The Animal Welfare Act, and the CDC/NIH's Biosafety in Microbiological and Biomedical Laboratories guide.

3. Results

3.1. COVAX-19 vaccine design and production

Based on the high binding score (-57.6 kcal/mol) seen from docking our 3D-model of spike protein to several putative receptors, we predicted ACE2 as the human entry receptor for SARS-CoV-2 (Fig. 1B) [24]. This was confirmed by other groups using in vitro assays [19]. Based on this spike protein model, we designed a stable soluble secreted spike protein trimer for use as the vaccine immunogen. We designed a synthetic gene comprising the spike protein extracellular domain (ECD) together with N-terminal honeybee melittin signal sequence (HBMss) to ensure protein secretion and attached a hexa-histidine tag at the C-terminal end to assist with protein purification (Fig. 1A). Molecular dynamic simulation performed on the spike protein ECD vaccine construct confirmed its ability to form a stable trimer despite the lack of the transmembrane and cytoplasmic domains and the absence of any large trimerisation domain tag as used by others (Fig. 1C). The spike ECD gene construct was constituted into a baculovirus backbone, and the subsequent virus then used to transfect two insect cell lines (SF9 and Tni). While both cell lines successfully secreted the protein construct, higher protein expression was obtained in the Tni cells and these were used for subsequent production of the recombinant spike protein which was purified using a nickel affinity column and sterile filtration. The final protein

product had a purity of ~ 90% by SDS-PAGE (Fig. 1**D & E**) and was sterile with a low endotoxin and residual DNA content (data not shown).

3.2. COVAX-19 vaccine induces spike protein RBD-binding and neutralising antibodies in mice

The serum anti-spike protein response of BL6 mice immunised with rSp alone was dominated by IgG1, a T helper 2 (Th2) isotype, whilst in Advax-SM adjuvanted groups the response was characterised by a switch to more IgG2b/c and IgG3 against spike (Fig. 2**B)**. Overall, Advax-SM adjuvant was associated with a much higher anti-spike IgG2/IgG1 ratio consistent with a Th1-biased response (Fig. 2**C)**. To provide an adjuvant comparison, we set up an additional study to compare the effects of the Advax-SM adjuvant to a traditional aluminium hydroxide adjuvant (Alhydrogel). As expected, the Alhydrogel adjuvant exacerbated the IgG1 (Th2) bias seen with rSp alone, thereby contrasting with the IgG2/3 (Th1) bias of the Advax-SM adjuvant. Most strikingly, mice immunised with Advax-SM adjuvanted rSp demonstrated high levels of *in vivo* cytotoxic T lymphocyte (CTL) killing of spike-labelled target cells, whereas mice immunised with rSp alone or formulated with Alhydrogel demonstrated minimal CTL activity against spike-labelled targets consistent with their Th2 immune bias (**Supplementary** Fig. 1).

Spike RBD-binding antibodies have been reported to correlate with SARS-CoV-2 virus neutralisation [29]. There was a high correlation for each IgG subclass between the level of spike and RBD binding antibodies by ELISA, suggesting a significant proportion of spike antibodies induced by our rSp antigen were directed against the RBD region. RBD-binding IgG was almost undetectable in mice immunised with rSp alone, although these mice did exhibit some RBD-binding IgM. Notably, the Advax-SM adjuvant increased the spike IgG response but particularly favoured production of RBD-binding antibodies when expressed as a ratio of the total spike IgG response (Fig. 2**C)**.

BALB/c mice, which have an overall Th2 bias, exclusively made IgG1 when immunised with rSp alone. Similar to what was seen in BL6 mice, in BALB/c mice Advax-SM adjuvanted rSp induced a switch from anti-spike IgG1 to IgG2b/c and IgG3 production The increased IgG2b/c and IgG3 induced by the Advax-SM adjuvant was equivalent to the reduction in IgG1. Interestingly, BALB/c mice had a low ratio of RBD to spike IgG, with IgM the dominant RBD-binding antibody, rather than IgG. This contrasted with the high RBD to spike IgG ratio seen in the BL6 mice (**Supplementary** Fig. 2).

To determine whether the spike antibodies induced by our vaccine could neutralise virus infectivity, immune sera were tested in both a pseudotyped lentivirus assay (pseudovirus assay) and a SARS-CoV-2 neutralisation assay (live virus assay). BL6 mice immunised with rSp 1 μg with Advax-SM adjuvant showed significantly higher pseudovirus neutralisation titres (GMT 320) compared to BL6 mice immunised with an equivalent dose of spike protein alone (GMT 140) (Fig. 3**A)** whereas BALB/c mice immunised with 1 μg rSp showed similar levels of pseudovirus neutralisation regardless of the presence of adjuvant.

Both BL6 and BALB/c mice immunised with Advax-SM adjuvanted rSp produced antibodies able to neutralise live SARS-CoV-2 virus. In BL6 mice, the highest neutralising antibodies were seen after immunisation with rSp 5 μg + Advax-SM (GMT 3,712), then rSp 1 μg with Advax-SM (GMT 1088) and then rSp alone (GMT 736) (Fig. 3**B)**. The same trends were seen in BALB/c mice with highest response for rSp 5 μg + Advax-SM (GMT 4,352), then rSp 1 μg with Advax-SM (GMT 960) and finally rSp alone (GMT 512). To evaluate potential cross-protection against a variant strain, sera were also tested for ability to neutralise the Alpha variant of concern (lineage B.1.1.7, or "UK-strain"). Only sera from BL6 or

BALB/c mice immunised with Advax-SM adjuvanted rSp were able to neutralise the B.1.1.7 variant virus, with no neutralisation activity seen in mice immunised with rSp alone (Fig. 3**C)**.

We next asked whether there was any correlation between total spike or RBD antibody levels and pseudotype or live virus neutralisation titres. In BL6 mice, there was a positive correlation between spike and RBD binding IgG and pseudotype and live virus neutralisation titres, with the highest correlation between spike IgG and pseudotype neutralisation (r^2 = 0.49, p < 0.0035), followed by RBD IgG and pseudotype neutralisation (r^2 = 0.38, p < 0.015) (**Supplementary** Fig. 3A). Interestingly, there were only weak non-significant correlations between spike IgG and live virus neutralisation titres (r^2 = 0.20, p < 0.09) or RBD IgG (r^2 = 0.22, p < 0.07).

In BALB/c mice, there was a positive correlation for spike IgG with pseudotype neutralisation titres (r^2 = 0.46, p < 0.005) (**Supplementary** Fig. 3B). There was also a positive correlation for spike IgM with both pseudotype (r^2 = 0.42, p < 0.009) and live virus (r^2 = 0.4, p < 0.01) neutralisation. However, there was no correlation between RBD IgM and either pseudotype or live virus neutralisation, suggesting that IgM in BALB/c might neutralise SARS-CoV-2 through an RBD-independent mechanism.

Interestingly, there was only a weak correlation between pseudotype and live virus neutralisation (r^2 = 0.17, p < 0.02) (**Supplementary** Fig. 4). This could reflect that pseudotype neutralisation assays are unique at two levels, they utilise greater numbers of viral particles to enable cellular transduction and GFP expression, and only measure the consequence of a single round of spike-driven cellular fusion. By contrast, the live virus neutralisation assay measures inhibition of viral entry and productive infection over a 3-day period with repeated rounds of viral replication. Hence, each assay measures different but important parameters of viral infection, providing clues as to the ability of immune sera to neutralise first-round viral entry vs. a replicative infection

3.3. Vaccine-induced T cell responses in mice

Cytokine production was measured in culture supernatants of rSp-stimulated splenocytes obtained from immunised mice. In BL6 mice, rSp-stimulated IL-2, IFN-γ and TNF-α was significantly higher in the Advax-SM group, consistent with their Th1 bias (Fig. 4**A-C)**. Similarly, in BALB/c mice, there was higher rSp-stimulated IFN-γ and TNF-α in the Advax-SM group (Fig. 4**A-C)**. In BALB/c mice, rSp-stimulated IL-4, IL-6 and IL-10 production was highest in the rSp-alone immunised group, which also exhibited low IFN-γ and TNF production, consistent with a Th2 bias (Fig. 4**D-F)**. IL-17 was modestly increased in Advax-SM adjuvanted rSp groups in both BL6 and BALB/c mice (Fig. 4**G)**. Overall, rSp-alone groups exhibited a Th2 cytokine bias, while Advax-SM groups exhibited a Th1 bias with an increased IFN-γ/IL-4 ratio (Fig. 4**H)**. ELISPOT assays on splenocytes from immunised mice confirmed significantly higher frequencies of IL-2 and IFN-γ secreting T cells in response to rSp stimulation in the Advax-SM groups (Fig. 5**A-B)**. Anti-spike IL-4-producing T cells were significantly higher in BALB/c mice, consistent with their Th2 bias (Fig. 5**C)**. Anti-spike IL-17-producing T-cells were also higher in the Advax-SM group in BL6 mice (Fig. 5**D)**.

Spike-specific CD4 + and CD8 + T cell memory cell proliferative responses were further assessed by CFSE-dye dilution after rSp stimulation. Notably, anti-spike CD8 T cell responses were markedly increased in both BALB/c and BL6 mice that had received Advax-SM adjuvanted rSp (Fig. 6), consistent with the high levels of anti-spike CTL activity also seen in mice receiving this formulation (**Supplementary** Fig. 1). There was also a clear trend to higher anti-spike CD4 T cell responses in mice that had received Advax-SM adjuvanted rSp, although this difference only reached significance in the BALB/c group (Fig. 6).
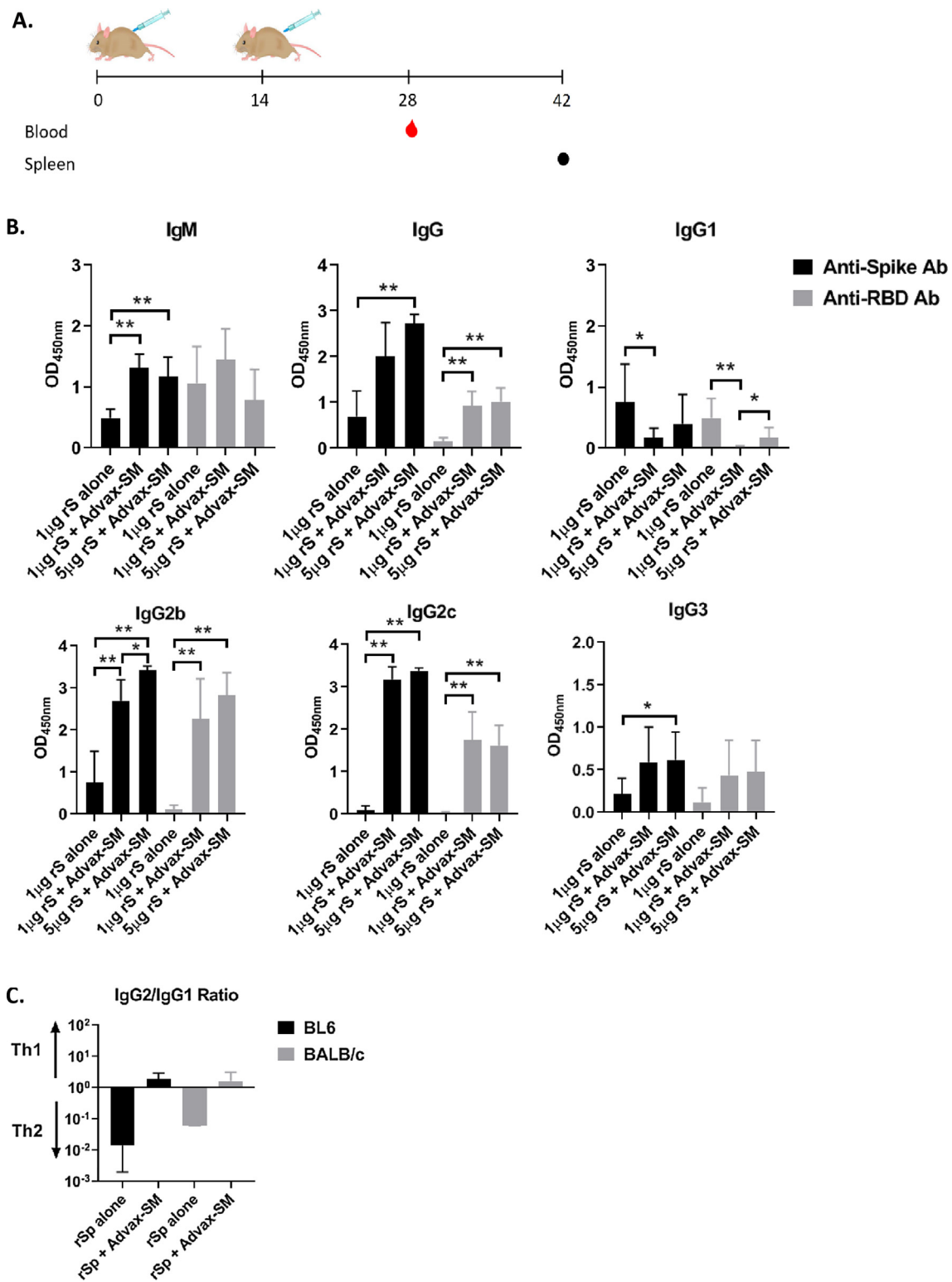
Fig. 2. Advax-SM adjuvant enhances total Spike and RBD antibodies. (A) Schematic diagram of immunisation and sample collection. Female C57BL/6 and BALB/c mice were immunised i.m. twice at 2-week intervals with 1 µg rSp or 1 and 5 µg rSp with Advax-SM adjuvant. Blood samples were collected 2 weeks later and spleens 3–4 weeks after the last immunisation. (B) Shown are ELISA results (mean + SD) in BL6 mice. Statistical analysis by Mann-Whitney test. *; p < 0.05, **; p < 0.01, ns; not significant. (C) Overview of IgG2/IgG1 ratio in BL6 and BALB/c mice.

### 3.4. Vaccine protection in ferrets

Having confirmed that the formulation of rSp with Advax-SM adjuvant gave optimal immunogenicity as measured by neutralis-

ing antibody, T cell cytokines and CTL responses in mice, we next tested vaccine efficacy in a ferret infection challenge model. Ferrets were given two immunisations 2 weeks apart with either of three dose levels of rSp protein (50, 25, or 12.5 µg) all formulated with

A. Neutralisation against SARS-CoV-2 Pseudovirus
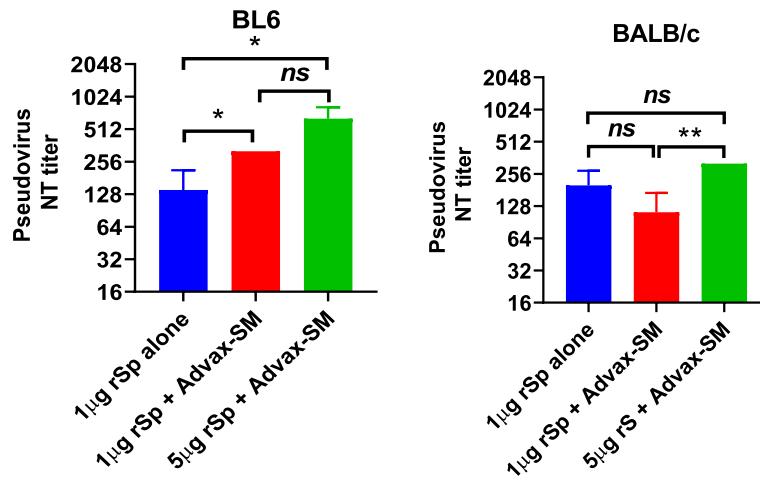
B. Neutralisation against live SARS-CoV-2 wild type virus (B.1.319)
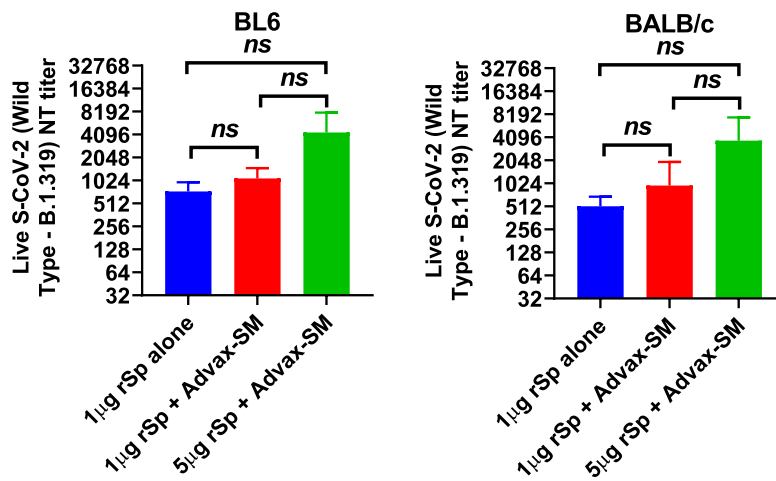
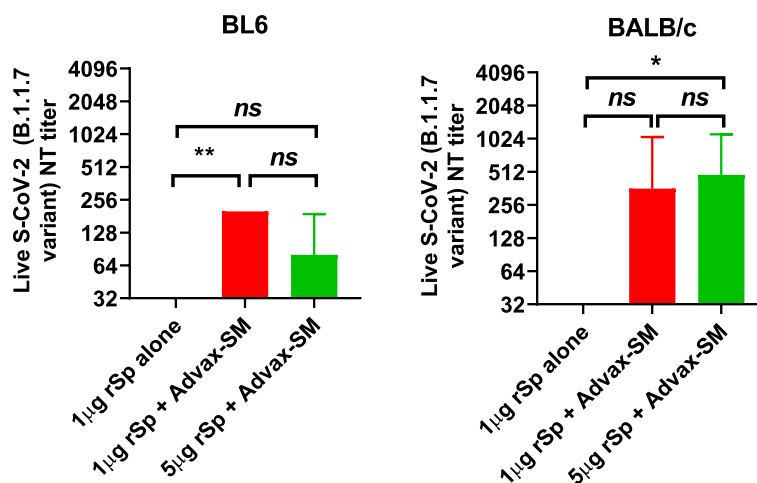**C.** Neutralisation against live SARS-CoV-2 alpha variant virus (lineage B.1.1.7)

Fig. 3. Neutralisation antibody titres from sera of immunised BL6 and BALB/c mice determined by (A) SARS-CoV-2 Spike pseudotyped lentivirus assay, (B) live SARS-CoV-2 wild type virus (lineage B.1.319) and (C) live SARS-CoV-2 variant of concern "Alpha" virus (lineage B.1.1.7, or "UK-strain"). Statistical analysis by Mann-Whitney test. *; $p < 0.05$, **; $p < 0.01$, ns; not significant.
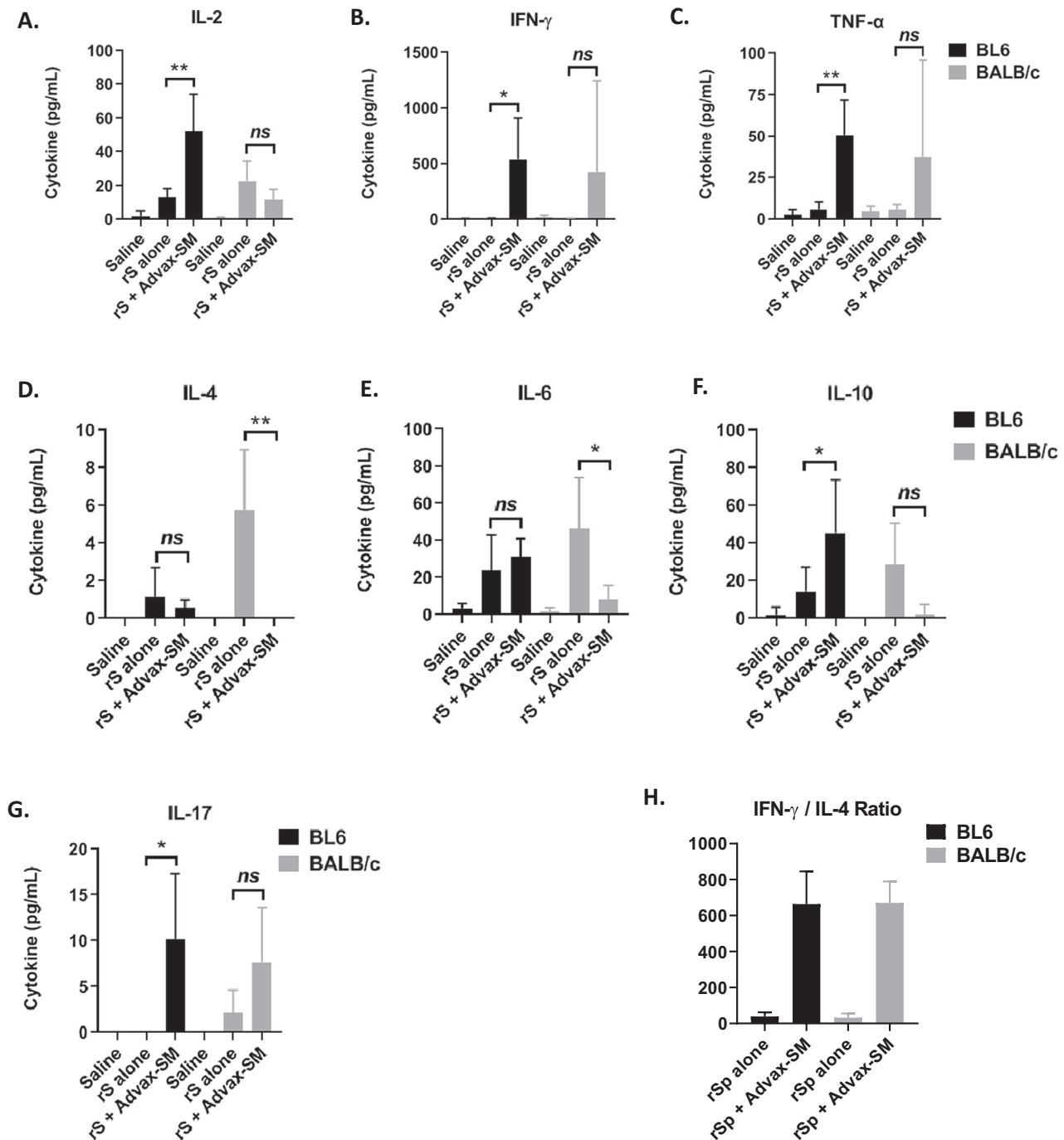
Fig. 4. Advax-SM adjuvant enhances cytokine production in response to rSp stimulation. Mice were immunised intramuscularly two times at 2 weeks apart with 1 µg rSp antigen alone or together with Advax-SM adjuvant. Cytokines produced by splenocytes that have been collected 2 or 3 weeks after the last immunisation then cultured 2 days with rSp antigen were determined by CBA assay. IL-2 (A), IFN-γ (B), TNF-α (C), IL-4, (D) IL-6 (E), IL-10 (F), IL-17 (G). Also shown is IFN-γ/IL-4 ratio as reflection of Th1/Th2 balance (H).

the same dose of Advax-SM adjuvant, with control groups receiving two doses of an irrelevant influenza vaccine with Advax-SM (adjuvant control), two doses of saline (saline control) or a single dose of rSp 50 µg + Advax-SM (single dose control) (Fig. 7A).

Sera was obtained 2 weeks after the first and second immunisation and measured for IgG to RBD. Anti-RBD IgG was detectable even 2 weeks after the first dose in all rSp-immunised groups and levels were further increased 2 weeks after the second dose in those animals that received the second rSp dose (Fig. 7B). Control groups had negligible RBD titres at all time points. Two weeks after the second dose there was no significant effect of rSp dose

seen on RBD titres being similar for the animals that had received either the 50, 25, or 12.5 µg doses.

In response to the nasal virus challenge, the ferrets showed minimal clinical signs of SARS-CoV-2 infection (**Supplementary** Fig. 5A). At 3 days post infection, lungs were harvested from three ferrets per group and scored for cellular infiltration and injury. Mock-vaccinated ferrets demonstrated a trend towards higher interstitial pneumonia based on H&E staining, and viral antigen was detectable in lung cells by immunohistochemistry (**Supplementary** Fig. 5B and Fig. 7Cxii). Ferrets that received just a single vaccine dose similarly showed a trend toward higher interstitial
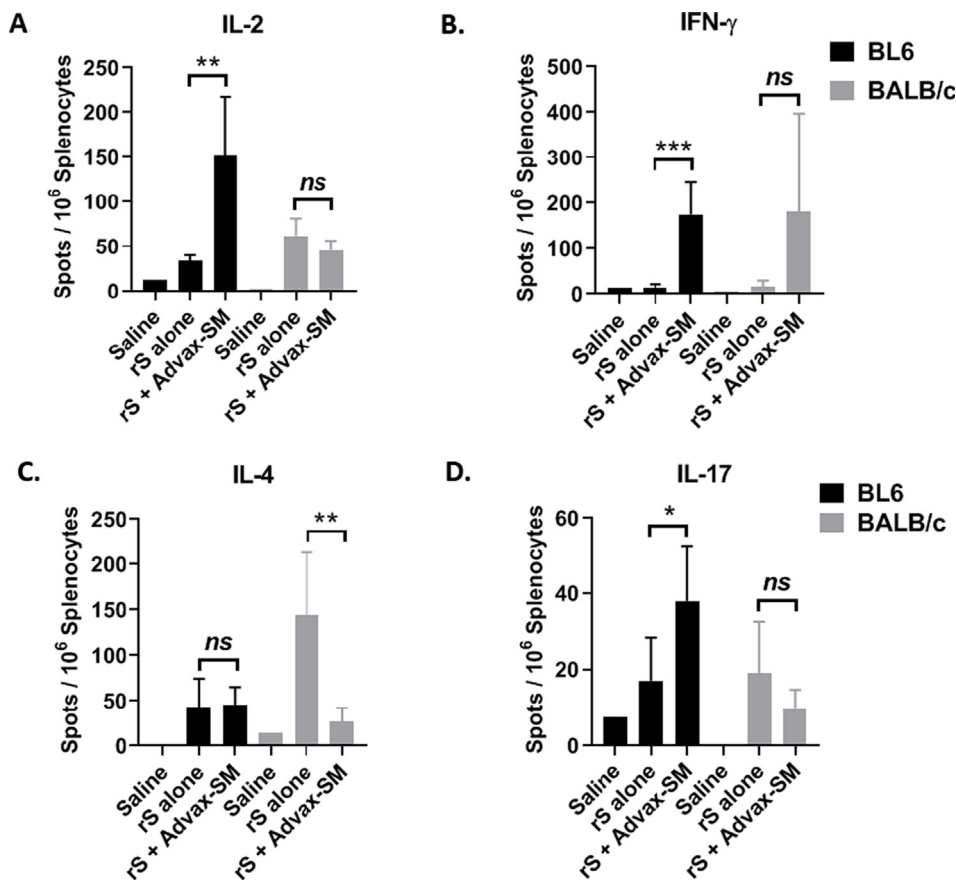
Fig. 5. Antigen-specific cytokine-producing T cells were evaluated by ELISPOT following stimulation of splenocytes with rSp. Statistical analysis was done by Mann-Whitney test. *; p < 0.05, **; p < 0.01, ***; p < 0.001, ns; not significant.
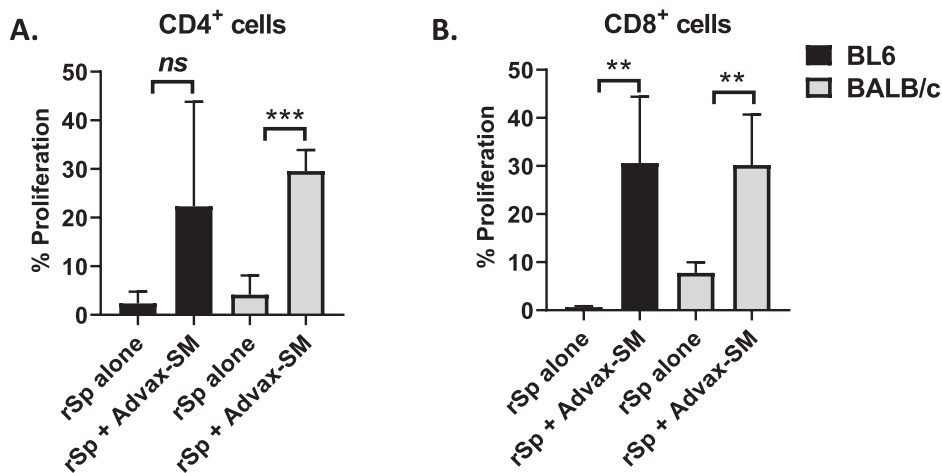

Fig. 6. Antigen-specific CD4+ and CD8+ T cell proliferation was measured by FACS using CFSE-labelled splenocytes harvested from immunised BL6 or BALB/c mice after culture for 5 days with rSp antigen. Results are presented as mean + SD. Statistical analysis was done by Mann-Whitney test. *; p < 0.05, **; p < 0.01, ***; p < 0.001, ns; not significant.

pneumonia in the H&E staining and positive virus staining (**Supplementary** Fig. 5B and 7Cxi). By comparison, all groups that received two doses of rSp with Advax-SM had negative SARS-CoV-2 virus staining in the lungs consistent with protection (Fig. 7-Cviii-x).

Next virus load was assessed in day 3 post-challenge nasal washes. Ferrets that received two immunisations of rSp at 25 µg

or 50 µg with Advax-SM adjuvant had no detectable nasal virus as measured by TCID$_{20}$ assay. Similarly, 5 out of 6 (84%) of the ferrets that received two immunisations at the lowest 12.5 µg rSp dose had no detectable virus in their nasal washes, day 3 post-challenge. By contrast, 50% of ferrets in the control and single dose groups had detectable virus in their nasal washes, day 3 post-challenge.
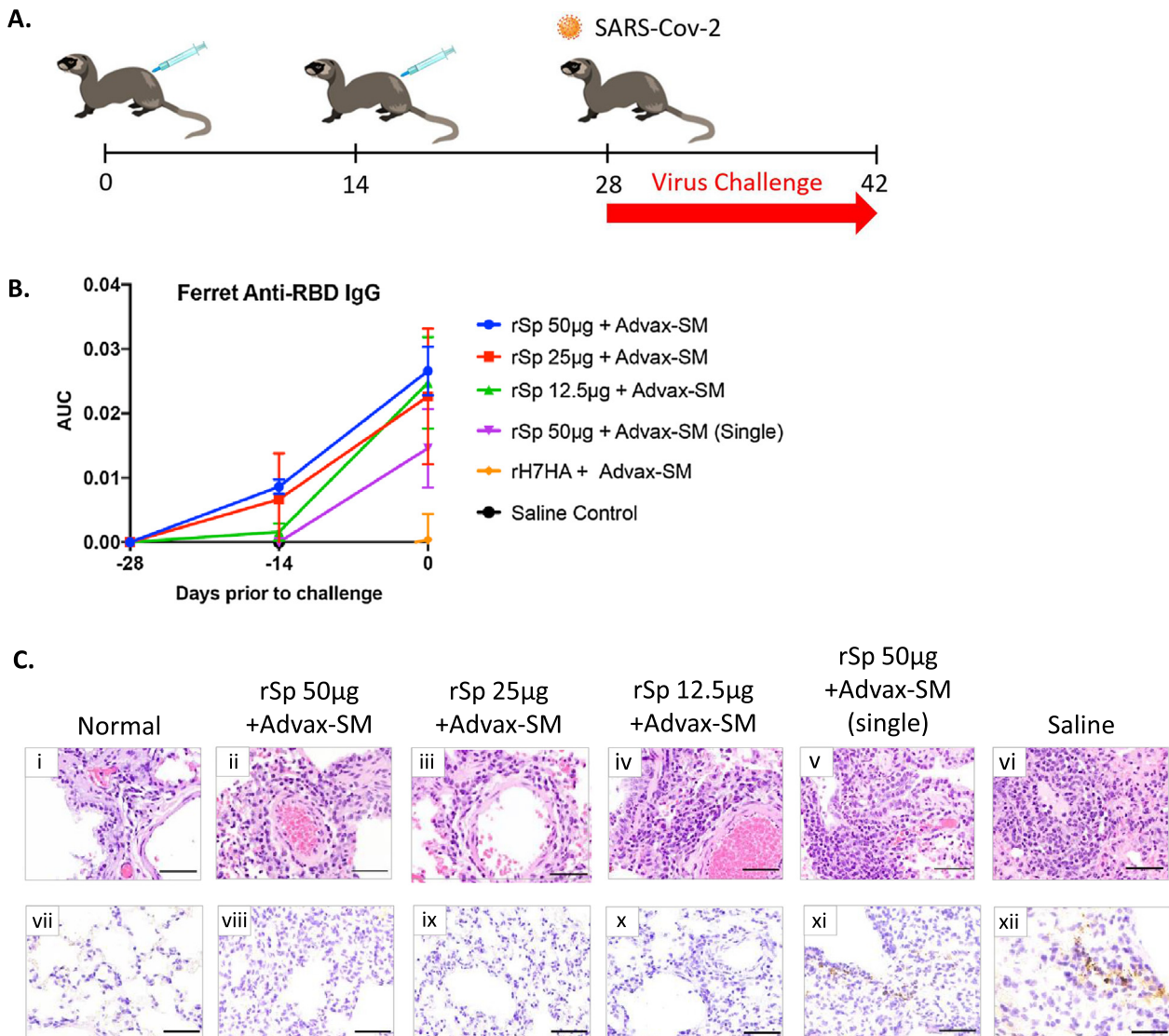
Fig. 7. Ferret SARS-CoV-2 Challenge Model. (A) Overview of Ferret study design. Ferrets (n = 6) were vaccinated at day 0 and boosted at day 14 with SARS-CoV-2 spike protein (12.5, 25 or 50 μg) formulated with 15 mg Advax-SM adjuvant. Control ferrets either received saline only (n = 3) or were immunised with influenza vaccine formulated with Advax-SM as a control (n = 3). Ferrets were challenged with SAR-CoV-2 virus (1 X 10^5 PFU) 14 days after last immunisation. Blood was collected at day − 28, −14. Lungs were collected 3 days post challenge for immunopathology. Lungs and nasal washes were collected 3 days post challenge for viral titres. (B) ELISA for Ferret anti-RBD IgG antibodies. (C) Haematoxylin & Eosin (H&E) (i-vi) and anti-SARS-CoV-2 nucleoprotein immunohistochemistry (IHC) staining (vii-xii) at 40x magnification (scale bar = 50 μm).

4. Discussion

Vaccines normally take 10–15 years from discovery to final market approval [30]. To accelerate our COVID-19 vaccine development we made use of a well-validated protein manufacturing platform complemented by *in silico* modelling analyses. In this way, as soon as the SARS-CoV-2 genome sequence became available in Jan 2020 [20], we were able to identify the putative spike protein, model its structure and use docking programs to predict human ACE2 as the main receptor for the virus, a finding confirmed by others [24]. This facilitated our rapid design of a recombinant spike protein antigen able to be produced as a soluble secreted protein in insect cells, which we named Covax-19™ vaccine.

We first evaluated the immunogenicity of Covax-19 vaccine in BL6 and BALB/c mice. Spike protein alone induced antigen-specific IgG and IgM antibodies with neutralisation activity as measured by pseudotype and wildtype virus neutralisation assays. This indicated the recombinant vaccine antigen produced using the insect cell-based baculovirus expression vector system (BEVS) was

a good immunogen. The benefits of BEVS is that it enables eukaryotic-like glycosylation whilst mitigating the risk of adventitious virus contamination associated with mammalian cell systems, provides high yields, and can be rapidly scaled [31] to respond to pandemic needs for rapid vaccine production. However, immunisation with spike protein alone induced a Th2 biased antibody response and induced only a weak T-cell response, indicating the need for an appropriate adjuvant

Advax-SM adjuvant has been under development by our team for some time and has shown utility in vaccines against other coronaviruses, namely SARS and MERS [14,15]. In the current study, the addition of Advax-SM to recombinant spike protein increased antibody production, created a more balanced Th1/Th2 response, induced cytotoxic T cells able to kill spike protein labelled targets and enhanced antibody neutralization. Notably, sera from Covax-19 immunised mice were able to cross-neutralise the B.1.1.7 variant of concern. This confirmed Advax-SM as a suitable adjuvant for the Covid-19 vaccine. Given the need for speed in development of this Covid-19 vaccine we did not conduct an extensive comparison

of other adjuvants with our spike protein, and most were either not available for commercial vaccine use, not available as GMP products, or were too experimental and not yet shown to be safe and effective in humans.

SARS-CoV-1 and SARS-CoV-2 viruses target interferon pathways to assist their immune escape [32,33]. Hence, coronavirus vaccines should ideally prime a strong memory Th1 and interferon response and induce CD8 + T cells to detect and kill virus-infected cells [34]. In mice, the Advax-SM adjuvated rSp vaccine induced a strong Th1 response characterised by a switch from IgG1 to IgG2 and IgG3 IgG isotypes, increased IL-2, IFN-γ and TNF-α secreting anti-spike T cells, and CTL killing of spike-labelled target cells. By contrast, immunisation with rSp alone (or formulated with alum adjuvant) induced a predominantly Th2 antibody and T cell response against spike protein, with lower levels of neutralising antibody against the wildtype virus and no neutralising activity against the B.1.1.7 virus variant and no *in vivo* CTL activity against spike-labelled targets.

Immunisation with Advax-SM adjuvanted rSp induced a high frequency of spike-specific memory CD4 + and CD8 + T cells, which were not seen in mice immunised with rSp alone. This suggests that the Advax-SM adjuvant was able to induce effective dendritic cell cross-presentation of spike protein to CD8 T cells, with CD8 T cell priming to exogenous antigens typically requiring activation of CD8 + dendritic cells [35]. Notably, this CD8 T cell cross-presentation was associated with significant *in vivo* CTL activity against spike-labelled targets suggesting that our vaccine should be able to robustly control infection, not just through induction of neutralising antibody but also through induction of CTLs able to efficiently identify and kill any residual virus-infected cells in the body. It has been difficult to identify non-reactogenic adjuvants that induce strong CD8 + T cell responses making this a potential key advantage of Advax-SM when used in viral vaccines where strong CD8 + T cell responses are likely to be important to protection. Overall, this demonstrated that our insect cell expressed spike ECD construct when formulated with Advax-SM adjuvant is an effective vaccine against SARS-CoV-2.

Whereas other adjuvant platforms might provide some non-specific antiviral protection via activation of the innate immune system, this has not been a feature of the Advax-SM adjuvant. Notably, there was no suggestion of disease reduction in the ferrets that were injected with Advax-SM adjuvant plus an irrelevant influenza vaccine. Similarly, in a past SARS CoV vaccine study we did not see any nonspecific protection in mice that received Advax-SM alone [14], nor did we see nonspecific protection of Advax-CpG adjuvant in a ferret H5N1 influenza study [36]. Hence, this data all supports the enhanced protection of Advax-SM adjuvanted Covid-19 vaccine being mediated by its ability to enhance the adaptive immune response to the co-administered spike antigen.

The role of RBD-binding and neutralising antibodies in SARS-CoV-2 protection remains unclear. Initially, there were concerns of the possibility of antibody-mediated disease enhancement (ADE), as seen in SARS, dengue, Respiratory Syncytial Virus and other viral diseases [37]. Reassuringly to date, there have been no reports of ADE in COVID-19 patients, although those with the most severe COVID-19 illness often have high RBD and neutralising antibodies [38], suggesting neutralising antibody may not be enough and other mediators like CTLs may also be required to fully control SARS-CoV-2 infection. Furthermore, a spike protein vaccine using a large Human Immunodeficiency Virus-derived protein trimerization tag and formulated with MF59 squalene adjuvant was shown to induce serum neutralising antibody, but provided no protection against nasal virus replication in either the ferret or hamster challenge models [39]. This suggests, at a minimum,

that serum neutralising antibody is not able to prevent nasal virus replication. Furthermore, convalescent plasma has not proved effective when administered to severely ill patients but instead can induce immune escape variants [40]. Hence antibodies by themselves may not be sufficient to prevent or reverse COVID-19 disease. In Phase 2 trials, LY-CoV555, a cocktail of two IgG1 antibodies appeared to accelerate the decline in viral load over time but ultimately did not demonstrate clinical benefit [41] with other experimental monoclonal treatments still undergoing human testing [42].

The gold standard for antibody assessment remains live wild-type virus neutralisation assays, as these directly measure the ability of antibody to block cellular infection. However, different cell types may be infected via different mechanisms, so use of different cell lines in these assays could still give varying results. VeroE6 is frequently used in virus neutralisation assays with viral entry in these cells primarily endosomal and driven through cathepsin cleavage of the spike protein. In contrast, entry of SARS-CoV-2 into nasopharyngeal cells is driven through TMPRSS2-mediated cleavage of spike [43]. Whilst primary ciliated or goblet cells from nasopharyngeal tissue might be the most physiologically relevant cell type to use in neutralisation assays, high-throughput serology screening using air-interface cultures is not feasible. Whilst pseudotyping assays can be performed outside of a BSL3 facility, they measure only a single round of spike-mediated cellular fusion and, hence, do not mimic a natural infection where there are multiple rounds of entry and replication. RBD-binding antibody assays work on the presumption that antibodies that block spike protein from binding to ACE2 should stop virus infectivity. However, in animal studies vaccines that have been shown to induce anti-RBD IgG titres have not prevented virus replication in the nasal mucosa, suggesting either that such antibodies fail to prevent virus binding or entry or that they fail to get access to the nasal epithelium.

How do results compare for these assays? Previous studies on convalescent patients have reported a positive correlation between spike-specific IgG and both pseudotype virus and live virus neutralisation. In our study, there was a poor correlation between the pseudovirus and live virus assays, suggesting they measure different determinants of neutralisation. The live virus assay measures the ability to block cell infection by a small pool of viral particles across 3 days of culture. The pseudotype assay uses a large pool of virus particles as a surrogate for a single spike-driven fusion event. In our study, total spike antibody ELISA predicted pseudotype neutralisation better than the RBD-binding ELISA. Interestingly, in BALB/c but not BL6 mice, there was a positive correlation between total anti-rSp IgM (but not anti-RBD IgM) with neutralisation titres. Elite donors with high neutralisation titres in human convalescent cohorts surprisingly achieved this via anti-viral IgM (S. Turville, personal communication). There is still no established correlate of COVID-19 protection that has been confirmed in either animal models or humans. The fact that different assays seem to yield different results suggests that the identification of a correlate based upon simple antibody protection may not be straightforward.

Unless a vaccine is able to induce potent sterilising immunity, some SARS-CoV-2 virus will inevitably enter cells in the nasal mucosa, where antibodies will not be able to reach it, and the virus will begin to replicate. A strong CD8 T cell response with interferon production and CTL activity is likely to be important for virus control in these circumstances. A large body of clinical data demonstrates that reduced T-cell responses and production of Th1 cytokines such as interferon and IL-2 are seen in patients with severe COVID-19 disease [44-47]. Moreover, the mode of action and protection of several SARS-CoV-2 vaccines has been linked to

induction of type I interferon secretion by amplifying T cell memory formation and promoting B cell differentiation and survival [48]. Notably, our Covax-19 vaccine imparted a strong Th1 bias and robust T cell responses by virtue of the Advax-SM adjuvant. By contrast, alum and squalene emulsion adjuvants induce a strong Th-2 bias, which may not be as beneficial for COVID-19 virus control [49]. COVID-19 vaccine with alum adjuvant demonstrated a Th2-biased response with a low IFN-γ/IL-4 ratio [50], and we similarly saw a strong Th2 bias of alum for spike protein in the current study. Notably, alum- and squalene-adjuvanted COVID-19 vaccines were both ineffective against nasal virus replication [39]. This contrasts strongly, with the ferret protection data shown here where Advax-SM adjuvanted rSp completely prevented both lung and nasal virus replication, an exciting finding as prevention of nasal virus replication could be the key to prevention of virus transmission. We currently do not know the mechanism for the prevention of nasal virus replication in the ferrets by Advax-SM adjuvanted rSp, with the possibilities that is it due to CTL induced by the vaccine migrating to the nasal mucosa where they might then eradicate virus infected cells, or an ability of the adjuvant to induce neutralising antibodies with different functional properties that are better able to access the nasal environment and prevent infectivity of the virus, or both. Future studies will attempt to explore these mechanisms further.

A limitation of the current study was that ferrets do not exhibit weight loss or other signs of SARS-CoV-2 clinical infection [51], with no animal models fully reproducing the features of severe SARS-CoV-2 clinical infection in humans. Ongoing studies are testing our Covax-19 vaccine in other species including hamsters and non-human primates to see whether the effects of the vaccine on inhibition of nasal virus replication extends to other species. The current study also only assessed short term protection and it will also be important in the future to assess long-term protection.

5. Conclusion

The COVID-19 pandemic represents a significant evolving global health crisis. The key to overcoming the pandemic lies in the development of an effective vaccine against SARS-CoV-2 that ideally should prevent transmission as well as prevent serious disease. Recombinant protein-based approaches to COVID-19 offer benefits over other technologies including a 40-year record of safety and effectiveness including in very young infants, together with reliable large scale manufacture and stability under refrigerated conditions [52]. By contrast, other available technologies, including nucleic acid and adenoviral vector platforms have a high level of reactogenicity and pose cold chain and other distribution challenges [53,54]. This study showed that an Advax-SM adjuvanted rSp vaccine (Covax-19 vaccine) when administered as two sequential intramuscular doses several weeks apart induces strong anti-spike antibody and T cell responses in mice and was able to protect ferrets against SARS-CoV-2 infection. The lack of day 3 nasal virus shedding in the immunised ferrets suggests Covax-19 vaccine may additionally be able to reduce virus transmission. Planned clinical trials will now assess how this promising animal data translates into human protection.

Declaration of Competing Interest

LL, NP, YHO, SP and JB are affliated with Vaxine which holds the rights to Covax-19 vaccine. The authors declare that they have no other known competing financial interests or personal relationships that could have appeared to influence the work reported in this paper.

Appendix A. Supplementary data

Supplementary data to this article can be found online at https://doi.org/10.1016/j.vaccine.2021.07.087.

References

[1] Hu B, Guo H, Zhou P, Shi Z-L. Characteristics of SARS-CoV-2 and COVID-19. Nat Rev Microbiol 2021;19(3):141–54.
[2] Weekly Operational Update on COVID-19. 2021.
[3] Gu J, Korteweg C. Pathology and pathogenesis of severe acute respiratory syndrome. The American journal of pathology. 2007;170(4):1136–47.
[4] Looi M-K. Covid-19: Is a second wave hitting Europe? BMJ 2020;371.
[5] Kupferschmidt K. Fast-spreading UK virus variant raises alarms. Science 2021;371(6524):9–10.
[6] Le TT, Cramer JP, Chen R, Mayhew S. Evolution of the COVID-19 vaccine development landscape. Nat Rev Drug Discov. 2020;19(10):667–8.
[7] Thanh Le T, Andreadakis Z, Kumar A, Gómez Román R, Tollefsen S, Saville M, et al. The COVID-19 vaccine development landscape. Nat Rev Drug Discov. 2020;19(5):305–6.
[8] van Riel D, de Wit E. Next-generation vaccine platforms for COVID-19. Nat Mater 2020;19(8):810–2.
[9] Coish JM, MacNeil AJ. Out of the frying pan and into the fire? Due diligence warranted for ADE in COVID-19. Microbes Infect 2020;22(9):405–6.
[10] Kostoff RN, Briggs MB, Porter AL, Spandidos DA, Tsatsakis A. COVID-19 vaccine safety. Int J Mol Med 2020;46:1599–602.
[11] Perrie Y, Mohammed AR, Kirby DJ, McNeil SE, Bramwell VW. Vaccine adjuvant systems: enhancing the efficacy of sub-unit protein antigens. Int J Pharm 2008;364(2):272–80.
[12] Pashine A, Valiante NM, Ulmer JB. Targeting the innate immune response with improved vaccine adjuvants. Nat Med 2005;11(S4):S63–8.
[13] Weinberger B. Adjuvant strategies to improve vaccination of the elderly population. Curr Opin Pharmacol 2018;41:34–41.
[14] Honda-Okubo Y, Barnard D, Ong CH, Peng B-H, Tseng C-T, Petrovsky N, et al. Severe acute respiratory syndrome-associated coronavirus vaccines formulated with delta inulin adjuvants provide enhanced protection while ameliorating lung eosinophilic immunopathology. J Virol 2015;89(6):2995–3007.
[15] Adney DR, Wang L, Van Doremalen N, Shi W, Zhang Y, Kong W-P, et al. Efficacy of an adjuvanted Middle East respiratory syndrome coronavirus spike protein vaccine in dromedary camels and alpacas. Viruses. 2019;11:212.
[16] Gordon DL, Sajkov D, Honda-Okubo Y, Wilks SH, Aban M, Barr IG, et al. Human Phase 1 trial of low-dose inactivated seasonal influenza vaccine formulated with Advax™ delta inulin adjuvant. Vaccine. 2016;34(33):3780–6.
[17] Gordon DL, Sajkov D, Woodman RJ, Honda-Okubo Y, Cox MMJ, Heinzel S, et al. Randomized clinical trial of immunogenicity and safety of a recombinant H1N1/2009 pandemic influenza vaccine containing Advax™ polysaccharide adjuvant. Vaccine. 2012;30(36):5407–16.
[18] Gordon D, Kelley P, Heinzel S, Cooper P, Petrovsky N. Immunogenicity and safety of Advax™, a novel polysaccharide adjuvant based on delta inulin, when formulated with hepatitis B surface antigen: a randomized controlled Phase 1 study. Vaccine. 2014;32(48):6469–77.
[19] Hoffmann M, Kleine-Weber H, Schroeder S, Krüger N, Herrler T, Erichsen S, et al. SARS-CoV-2 cell entry depends on ACE2 and TMPRSS2 and is blocked by a clinically proven protease inhibitor. Cell 2020;181(2):271–280.e8.
[20] Wu F, Zhao Su, Yu B, Chen Y-M, Wang W, Song Z-G, et al. A new coronavirus associated with human respiratory disease in China. Nature 2020;579(7798):265–9.
[21] Song W, Gui M, Wang X, Xiang Y. Cryo-EM structure of the SARS coronavirus spike glycoprotein in complex with its host cell receptor ACE2. PLoS Pathogens. 2018;14:e1007236.
[22] Wu K, Peng G, Wilken M, Geraghty RJ, Li F. Mechanisms of host receptor adaptation by severe acute respiratory syndrome coronavirus. J Biol Chem 2012;287(12):8904–11.
[23] Yan Y, Tao H, He J, Huang S-Y. The HDOCK server for integrated protein–protein docking. Nat Protoc 2020;15(5):1829–52.
[24] Piplani S, Singh PK, Winkler DA, Petrovsky NJapa. In silico comparison of spike protein-ACE2 binding affinities across species; significance for the possible origin of the SARS-CoV-2 virus. arXiv preprint. 2020;arXiv:2005:06199.

[25] Aggarwal A, Iemma TL, Shih I, Newsome TP, McAllery S, Cunningham AL, et al. Mobilization of HIV spread by diaphanous 2 dependent filopodia in infected dendritic cells. PLoS Pathog. 2012;8:e1002762.

[26] Toscano M G, Frecha C, Ortega C, Santamaría M, Martín F, Molina I J. Efficient lentiviral transduction of Herpesvirus saimiri immortalized T cells as a model for gene therapy in primary immunodeficiencies. Gene Ther. 2004;11 (12):956–61.

[27] Honda-Okubo Yoshikazu, Ong Chun Hao, Petrovsky Nikolai. Advax delta inulin adjuvant overcomes immune immaturity in neonatal mice thereby allowing single–dose influenza vaccine protection. Vaccine. 2015;33 (38):4892–900.

[28] Zhi Yan, Kobinger Gary P, Jordan Heather, Suchma Katie, Weiss Susan R, Shen Hao, et al. Identification of murine CD8 T cell epitopes in codon-optimized SARS-associated coronavirus spike protein. Virology 2005;335(1):34–45.

[29] Salazar E, Kuchipudi SV, Christensen PA, Eagar T, Yi X, Zhao P, et al. Convalescent plasma anti–SARS-CoV-2 spike protein ectodomain and receptor-binding domain IgG correlate with virus neutralization. The Journal of Clinical Investigation. 2020;130:6728-38.

[30] Fedson DS. Vaccine development for an imminent pandemic: why we should worry, what we must do. Human Vaccines. 2006;2:38-42.

[31] Kost Thomas A, Condreay J Patrick, Jarvis Donald L. Baculovirus as versatile vectors for protein expression in insect and mammalian cells. Nat Biotechnol 2005;23(5):567–75.

[32] Lei Xiaobo, Dong Xiaojing, Ma Ruiyi, Wang Wenjing, Xiao Xia, Tian Zhongqin, et al. Activation and evasion of type I interferon responses by SARS-CoV-2. Nat Commun 2020;11(1). https://doi.org/10.1038/s41467-020-17665-9.

[33] Lokugamage KG, Hage A, de Vries M, Valero-Jimenez AM, Schindewolf C, Dittmann M, et al. Type I interferon susceptibility distinguishes SARS-CoV-2 from SARS-CoV. Journal of Virology. 2020.

[34] Appay Victor, Douek Daniel C, Price David A. CD8+ T cell efficacy in vaccination and disease. Nat Med 2008;14(6):623–8.

[35] Ho NI, Raaijmakers TK, Adema GJ. Adjuvants enhancing cross-presentation by dendritic cells: the key to more effective vaccines? Frontiers in Immunology. 2018;9:2874.

[36] Layton RC, Petrovsky N, Gigliotti AP, Pollock Z, Knight J, Donart N, et al. Delta inulin polysaccharide adjuvant enhances the ability of split-virion H5N1 vaccine to protect against lethal challenge in ferrets. Vaccine. 2011;29:6242-51.

[37] Lee Wen Shi, Wheatley Adam K, Kent Stephen J, DeKosky Brandon J. Antibody-dependent enhancement and SARS-CoV-2 vaccines and therapies. Nat Microbiol 2020;5(10):1185–91.

[38] Chen Xiangyu, Pan Zhiwei, Yue Shuai, Yu Fei, Zhang Junsong, Yang Yang, et al. Disease severity dictates SARS-CoV-2-specific neutralizing antibody responses in COVID-19. Signal Transduction Targeted Therapy. 2020;5(1). https://doi.org/10.1038/s41392-020-00301-9.

[39] Watterson D, Wijesundara D, Modhiran N, Mordant F, Li Z, Avumegah M, et al. Molecular clamp stabilised Spike protein for protection against SARS-CoV-2.30

[40] September 2020, PREPRINT (Version 1) available at Research Square [https://doi.org/10.21203/rs.3.rs-68892/v1].

[41] Zeng Q-L, Yu Z-J, Gou J-J, Li G-M, Ma S-H, Zhang G-F, et al. Effect of convalescent plasma therapy on viral shedding and survival in patients with coronavirus disease 2019. The Journal of Infectious Diseases. 2020;222:38-43.

[42] Dyer O. Covid-19: Eli Lilly pauses antibody trial for safety reasons. BMJ. 2020;14:m3985.

[43] DeFrancesco Laura. COVID-19 antibodies on trial. Nat Biotechnol 2020;38 (11):1242–52.

[44] Sungnak Waradon, Huang Ni, Bécavin Christophe, Berg Marijn, Queen Rachel, Litvinukova Monika, et al. SARS-CoV-2 entry factors are highly expressed in nasal epithelial cells together with innate immune genes. Nat Med 2020;26 (5):681–7.

[45] Chen G, Wu D, Guo W, Cao Y, Huang D, Wang H, et al. Clinical and immunological features of severe and moderate coronavirus disease 2019. The Journal of clinical investigation. 2020;130:2620-9.

[46] Chua RL, Lukassen S, Trump S, Hennig BP, Wendisch D, Pott F, et al. COVID-19 severity correlates with airway epithelium–immune cell interactions identified by single-cell analysis. Nature biotechnology. 2020;38:970-9.

[47] Zheng Hong-Yi, Zhang Mi, Yang Cui-Xian, Zhang Nian, Wang Xi-Cheng, Yang Xin-Ping, et al. Elevated exhaustion levels and reduced functional diversity of T cells in peripheral blood may predict severe progression in COVID-19 patients. Cell Mol Immunol 2020;17(5):541–3.

[48] Lagunas-Rangel Francisco Alejandro, Chávez-Valencia Venice. High IL-6/IFN-γ ratio could be associated with severe disease in COVID-19 patients. J Med Virol 2020;92(10):1789–90.

[49] Teijaro John R, Farber Donna L. COVID-19 vaccines: modes of immune activation and future challenges. Nat Rev Immunol 2021;21(4):195–7.

[50] Gupta Tania, Gupta Shishir K. Potential adjuvants for the development of a SARS-CoV-2 vaccine based on experimental results from similar coronaviruses. Int Immunopharmacol 2020;86:106717. https://doi.org/10.1016/j.intimp.2020.106717.

[51] Qi X, Ke B, Feng Q, Yang D, Lian Q, Li Z, et al. Construction and immunogenic studies of a mFc fusion receptor binding domain (RBD) of spike protein as a subunit vaccine against SARS-CoV-2 infection. Chemical Communications. 2020;56:8683-6.

[52] Kim Young-Il, Kim Seong-Gyu, Kim Se-Mi, Kim Eun-Ha, Park Su-Jin, Yu Kwang-Min, et al. Infection and rapid transmission of SARS-CoV-2 in ferrets. Cell Host Microbe 2020;27(5):704–709.e2.

[53] Calina D, Docea AO, Petrakis D, Egorov AM, Ishmukhametov AA, Gabibov AG, et al. Towards effective COVID-19 vaccines: Updates, perspectives and challenges. Int J Mol Med 2020;46:3–16.

[54] Rollier Christine S, Reyes-Sandoval Arturo, Cottingham Matthew G, Ewer Katie, Hill Adrian VS. Viral vectors as vaccine platforms: deployment in sight. Curr Opin Immunol 2011;23(3):377–82.

[55] Leitner Wolfgang W, Ying Han, Restifo Nicholas P. DNA and RNA-based vaccines: principles, progress and prospects. Vaccine. 1999;18(9-10):765–77.